

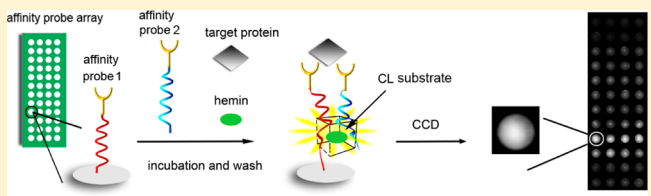
# Chemiluminescence Imaging for a Protein Assay via Proximity-Dependent DNAzyme Formation

Chen Zong,<sup>†</sup> Jie Wu,<sup>†</sup> Mengmeng Liu,<sup>†</sup> Linlin Yang,<sup>†</sup> Feng Yan,<sup>‡</sup> and Huangxian Ju<sup>\*,†</sup>

<sup>†</sup>State Key Laboratory of Analytical Chemistry for Life Science, School of Chemistry and Chemical Engineering, Nanjing University, Nanjing, Jiangsu 210093, P.R. China

<sup>‡</sup>Department of Clinical Laboratory, Nanjing Medical University Cancer Hospital and Jiangsu Cancer Hospital, 42 Baiziting Road, Nanjing, Jiangsu 210009, P.R. China

**ABSTRACT:** An array-based chemiluminescence (CL) imaging method is presented for simple and high throughput detection of protein targets via the formation of a proximity-dependent DNAzyme to produce sensitive CL signal. The protein array is prepared by covalently immobilizing single-stranded guanine-rich nucleic acid 1-labeled antibody 1 (GDNA1-Ab1) or GDNA-thrombin aptamer subunit 1 (Apt-P1) as the capture probe on each sensing site on an aldehyde-functionalized disposable glass chip. In the presence of target protein, hemin, and another GDNA2-Ab2 or Apt-P2 probe, a sandwich complex among the protein and two probes can be formed to trigger the proximity assembly of GDNA1, hemin, and GDNA2, which leads to the formation of hemin-G-quadruplex DNAzyme. At different sensing sites, the DNAzyme-induced CL signals are simultaneously collected by a charge-coupled device for imaging readout of the sensing events. As a proof of concept, the proposed array-based CL imaging strategy is applied to detect carcinoembryonic antigen and thrombin and shows wide linear ranges over 4 and 5 orders of magnitude with the detection limits of 0.15 ng mL<sup>-1</sup> and 0.49 pM, respectively. Benefiting from the one-step proximity-dependent DNAzyme formation, the assay method is extremely simple and can be carried out within 40 min. By using different probes, the array can be easily used to detect more protein analytes. The advantages of easy operation, short assay time, good sensitivity, and versatility make it a promising candidate for point-of-care testing and commercial application.



The detection of cancer biomarkers is of great significance in early clinical diagnosis and disease prevention.<sup>1</sup> Numerous immunosensors and immunoassay methods have been proposed to determine the biomarkers accurately,<sup>2,3</sup> most of which adopt sandwich detection format with enzyme linked probe for signal output.<sup>1,4,5</sup> To improve the detection sensitivity, different signal probes have been prepared by using micro- or nanomaterials such as gold nanoparticles,<sup>6–8</sup> gold nanorods,<sup>9</sup> carbon nanotubes,<sup>10–12</sup> magnetic beads,<sup>13</sup> graphene oxide,<sup>14,15</sup> and silica nanoparticles,<sup>16,17</sup> as carriers to load enzyme molecules for a single recognition event, and DNA-related amplification strategies including rolling circle amplification, nicking enzyme recycling amplification, and hybridization chain reaction have also been used to introduce multienzymes on each immunocomplex.<sup>18–22</sup> Although these assays show high detection sensitivity, the complex preparation and difficult storage of the probes as well as the rigorous conditions of DNA amplifications limit their practical applications.

Compared to natural enzymes, G-quadruplex/hemin DNAzyme, which offers the advantages of easy production and better stability and robustness, has attracted growing interest, and has been widely used in the design of sensitive immunoassays.<sup>20,23</sup> G-quadruplex/hemin DNAzyme formed by binding a G-quadruplex DNA strand with a hemin molecule can be conveniently in situ generated by various DNA assembly strategies. Particularly, the proximity-dependent recombination

of DNAzyme by using two fragments of G-quadruplex can efficiently avoid the nonspecific adsorption of the detection probes and thus provide a relatively low background.<sup>24–27</sup> This strategy has been implemented for chemiluminescent (CL) and CL resonance energy transfer detections of DNA, heavy ions, and cocaines<sup>28–30</sup> and construction of logic gates.<sup>31</sup> In these assays, the formed DNAzyme serves as the mimic of horseradish peroxidase to catalyze the oxidation of luminol by hydrogen peroxide<sup>29,30</sup> and generate the amplified CL signal. However, its application in detection of protein biomarkers still remains challenging.

Inspired by the proximity ligation assay (PLA),<sup>32</sup> a lot of target-induced DNA assembly strategies have recently been developed for protein detection.<sup>33–36</sup> These strategies achieve the DNA assembly through the sandwich immunoreaction among the target protein and two DNA labeled antibody (Ab) probes to produce the proximity effect for inducing the hybridization of two close DNA strands,<sup>33,35</sup> which are then followed with DNA amplification for enhancing the detection signal.<sup>37–43</sup> This work integrated the proximity assay and DNAzyme recombination strategy on a disposable chip to present an array-based chemiluminescence imaging assay

Received: July 24, 2014

Accepted: September 2, 2014

Published: September 2, 2014

Scheme 1. General Principle of the Array-Based Chemiluminescence Imaging Method with Proximity-Dependent Formation of DNAzyme

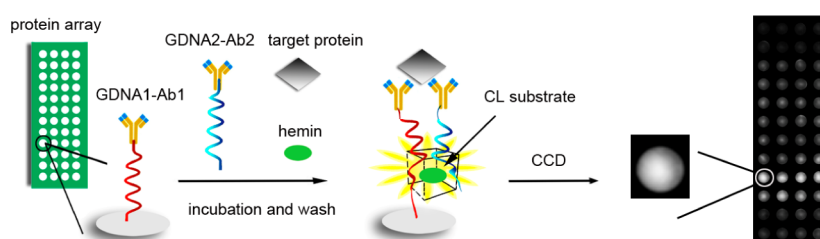


Table 1. Sequences of Oligonucleotides Used in This Work

oligonucleotides	sequences <sup>a</sup>
GDNA1	5'-COOH-A <sub>12</sub> GCAATCAAAA <b>GGGCAGGG</b> -C <sub>7</sub> -NH <sub>2</sub> -3'
GDNA2	5'- <b>GGGAGGTGAAA</b> ACTAACGA <sub>12</sub> -C <sub>3</sub> -SH-3'
Apt-P1	5'-TGGTTGGTGCAATCAAAA <b>GTGGAGGG</b> -C <sub>7</sub> -NH <sub>2</sub> -3'
Apt-P2	5'- <b>GGGACGGGAAA</b> ACTAACTGGTTGG-3'
B-GDNA3	5'-biotin-AGCAATCAAAA <b>GGGCAGGG</b> -3'
B-GDNA4	5'- <b>GGGAGGTGAAA</b> ACTAACGA-biotin-3'
G4 DNA	5'-TTTTTTGGGTTGGGCGGGATGGG-3'
Apt-P3	5'-TGGTTGGTGCAATCAAAA-C <sub>7</sub> -NH <sub>2</sub> -3'
Apt-P4	5'-AAA <b>ACTAACTGGTTGG</b> -3'

<sup>a</sup>The bold part represents the two split fragments of G-quadruplex.

(CLIA) method for simple and high throughput detection of protein targets. In order to realize the in situ formation of DNAzyme, the sequence of the peroxidase-mimicking DNAzyme was split into two fragments (guanine-rich nucleic acid 1, GDNA1, and guanine-rich nucleic acid 2, GDNA2), and each of them was conjugated with target-responsible Ab or aptamer for preparation of two affinity probes. One of the probes as the capture probe was immobilized on the sensing site of the disposable chip (Scheme 1). The presence of target antigen triggered the formation of sandwich immunocomplex and the proximity assembly of the two G-quadruplex fragments and hemin, which induced the in situ formation of the hemin-G-quadruplex DNAzyme on the sensing site. The DNAzyme-generated CL signals could be simultaneously collected by a charge-coupled device (CCD) for imaging assay of the targets. Benefiting from the one-step formation of DNAzyme, the proposed CLIA method was simpler and faster than previously reported array-based CL immunoassays.<sup>5,6,44,45</sup> The easy operation, short assay time, high sensitivity, acceptable accuracy, and good versatility of the array-based CLIA indicated its promising application in point-of-care testing.

## EXPERIMENTAL SECTION

**Materials and Reagents.** The oligonucleotides were synthesized and purified by Shanghai Sangon Biotechnology Co. Ltd. (China). Their sequences are shown in Table 1. Antibodies of carcinoembryonic antigen (anti-CEA, mouse monoclonal antibodies, clone Nos. Z-2011 and Z-2012) and standard solutions of CEA antigen were purchased from Beijing Keybiotech Co. Ltd. (China). Human  $\alpha$  thrombin was obtained from Tideradar Beijing Technology Co. Ltd. (China). CL substrate solution containing luminol-*p*-iodophenol and H<sub>2</sub>O<sub>2</sub> was obtained from Autobio Diagnostics Co. Ltd. (China). Hemin, streptavidin, *N*-hydroxysuccinimide (NHS), and 1-ethyl-3-(3-dimethylaminopropyl) carbodiimide-HCl (EDC) were purchased from Sigma-Aldrich Chemical Co. (St. Louis, MO). Hemin stock solution (1 mM) was prepared in DMSO

and stored in the dark at 4 °C. Sulfosuccinimidyl-4-(*N*-maleimidomethyl) cyclohexane-1-carboxylate (SMCC) was supplied by Heowns Biochem LLC (China). Dithiothreitol (DTT) was from Shanghai Sangon Biotechnology Co. Ltd. (China). Ultrapure water obtained from a Millipore water purification system ( $\geq 18$  M $\Omega$ , Milli-Q, Millipore) was used in all assays. All other reagents were of analytical grade and used without further purification.

TE buffer (10 mM Tris-HCl, containing 1 mM EDTA and 0.3 M NaCl, pH 7.9) was used for the preparation of oligonucleotide stock solutions. PBS1 (55 mM, containing 150 mM NaCl, 20 mM EDTA, pH 7.2) and PBS2 (55 mM, containing 150 mM NaCl, 5 mM EDTA, pH 7.2) were used to prepare the GDNA2-Ab2 probe. PBS3 (100 mM, pH 7.4) containing 10 mM ethanolamine or 0.1 M KCl was used as blocking buffer or dilution of hemin solution, respectively. Washing buffer was PBS3 spiked with 0.05% Tween-20. Tris-HCl buffer (20 mM, containing 8.5% glycerin, 5 mM K<sup>+</sup>, 100 mM Na<sup>+</sup>, 1 mM Ca<sup>2+</sup>, and 1 mM Mg<sup>2+</sup>, pH 7.4) was used for the preparation of stock solutions of thrombin and its aptamer. MES buffer (pH = 6.0) was used to dissolve EDC and NHS for connection of the amino group of labeled antibody 1 (Ab1) and the carboxyl group of GDNA1. The clinical serum samples were from Jiangsu Cancer Hospital (China). The electrochemiluminescent (ECL) immunoassay reagent kits for reference detection were provided by Roche Diagnostics GmbH (Germany).

**Apparatus.** Cooled low-light CCD with high resolution (BioImaging Systems Chemi HR 410 camera, UVP, USA) was used to collect the CL images. IFFM-E luminescent analyzer (Remax, China) was used for static CL detections. The circular dichroism (CD) spectra were obtained with a J-810/163-900 circular dichroism chiroptical spectrometer (Jasco, Japan). The control levels of CEA in sera were obtained with an automated ECL analyzer (Elecsys 2010, Roche).

**Fabrication of Protein Array.** The protein array contained 48 sensing cells in a 4 row  $\times$  12 column format. Briefly, a

pre-designed hydrophobic photoinactive film with 48 cells (4 mm diameter, 1 mm edge-to-edge separation) was fixed on an aromatic aldehyde-modified glass slide (Shanghai Baio Technology Co. Ltd., China). Six  $\mu\text{L}$  of 30 nM GDNA1 was then dropped on each cell and incubated overnight at 4 °C. The GDNA1 in TE buffer could be modified on the sensing cell through the interaction between amino group of DNA and aromatic aldehydes on glass<sup>46</sup> to form a stable aromatic Schiff base. After these sensing cells were thoroughly rinsed with washing buffer and the unreacted aldehyde groups were blocked with blocking buffer for 2 h, the carboxyl group of GDNA1 was activated with EDC and NHS for 50 min. Subsequently, 6  $\mu\text{L}$  of 10  $\mu\text{g mL}^{-1}$  capture anti-CEA (Ab1) was injected on the sensing site to link with GDNA1. After a washing process, the protein array for CEA was obtained. Similarly, the thrombin array was prepared by directly dropping 6  $\mu\text{L}$  of 30 nM GDNA-thrombin aptamer subunit (Apt-P1) on the sensing site to incubate overnight at 4 °C and then blocking with blocking buffer for 2 h. The obtained arrays were stored in PBS3 at 4 °C before use.

**Preparation of GDNA2-Ab2.** The GDNA2-Ab2 probe was prepared by a modified coupling procedure.<sup>47</sup> Ab2 (2 mg  $\text{mL}^{-1}$ ) was first reacted with a 20-fold molar excess of SMCC in PBS1 for 2 h at room temperature. The obtained Ab2-SMCC was purified by ultrafiltration using a 100 KD Millipore (10 000 rpm, 10 min). In parallel, 12  $\mu\text{L}$  of 100  $\mu\text{M}$  thiolated GDNA2 was reduced with 16  $\mu\text{L}$  of 100 mM DTT in PBS1 at 37 °C for 1 h. The reduced GDNA2 was purified by ultrafiltration using a 3 KD Millipore (10000 rpm, 10 min). Then, the resulting Ab2-SMCC and GDNA2 were mixed in 200  $\mu\text{L}$  of PBS2, incubated overnight at 4 °C, and purified by ultrafiltration using a 100 KD Millipore (10000 rpm, 10 min) for several times to remove the unreacted GDNA2. The obtained GDNA2-Ab2 was collected at a concentration of 6.0  $\mu\text{M}$  in PBS2, which was diluted with PBS2 at 100-fold prior to use.

**CLIA of CEA.** Two  $\mu\text{L}$  of CEA solution or serum sample was mixed with 2  $\mu\text{L}$  of 60 nM GDNA2-Ab2 and 2  $\mu\text{L}$  of 3  $\mu\text{M}$  hemin. The mixture was immediately added to the sensing site and incubated for 30 min at room temperature. After washing and drying, 6  $\mu\text{L}$  of CL substrate (luminol-*p*-iodophenol- $\text{H}_2\text{O}_2$ ) was delivered to the sensing site to trigger the CL reaction. The CL signals on all sensing sites of the array could be simultaneously recorded by CCD with a 5 min dynamic integration (Scheme 1) and automatically identified by VisionWorksLS image acquisition and analysis software (UVP). The CL intensity of each spot was calculated as the mean pixel intensity within a square of a given side length around each spot center. The protein array could be prepared with all or part of the cells, depending on the demand. To ensure the homogeneity of all cells for parallel sensing, the reaction solutions should be dropped on the cells as fast as possible.

**CLIA of Thrombin.** Similar to the CLIA of CEA, 2  $\mu\text{L}$  of thrombin was first mixed with 2  $\mu\text{L}$  of 100 nM Apt-P2 and 2  $\mu\text{L}$  of 3  $\mu\text{M}$  hemin. The mixture was incubated on the thrombin sensing site for 40 min at room temperature. After rinsing with washing buffer and drying, 6  $\mu\text{L}$  of CL substrate was added to obtain the CL image.

## RESULTS AND DISCUSSION

**Proximity-Dependent Formation of DNAzyme.** A typical streptavidin–biotin system was used to mimic the antibody–antigen affinity recognition and investigate the

proximity-dependent DNAzyme formation. A pair of biotinylated DNA sequences containing G-quadruplex fragments (B-GDNA3 and B-GDNA4) was designed as the probes. The mixture of B-GDNA3 and B-GDNA4 showed slight CD absorption (Figure 1A). In the presence of streptavidin, the

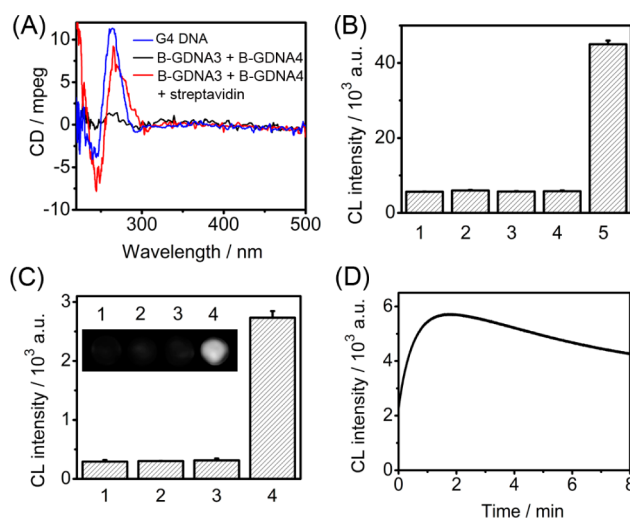


**Figure 1.** Experimental confirmation of the proximity-dependent formation of DNAzyme. (A) CD spectra at 2.5  $\mu\text{M}$ . (B) CL intensity of (1) hemin, the mixture of (2) B-GDNA3 and hemin, (3) streptavidin and hemin, (4) B-GDNA3, B-GDNA4, and hemin, and (5) B-GDNA3, B-GDNA4, streptavidin, and hemin at 160  $\text{ng mL}^{-1}$  CEA with the concentrations of 1.5  $\mu\text{M}$  for B-GDNA3, B-GDNA4, and streptavidin and 7.5  $\mu\text{M}$  for hemin. (C) CL spots of the CEA array incubated with hemin (1) and the mixtures of hemin and (2) 1.6  $\mu\text{g mL}^{-1}$  CEA, (3) 20 nM GDNA2-Ab2, and (4) 20 nM GDNA2-Ab2 and 1.6  $\mu\text{g mL}^{-1}$  CEA. (D) Kinetic curve of the CL reaction at 160  $\text{ng mL}^{-1}$  CEA.

mixture of B-GDNA3 and B-GDNA4 showed two obvious CD absorptions at 240 and 265 nm, which were attributed to those of complete G-quadruplex DNA (G4 DNA).<sup>48</sup> This phenomenon indicated the specific affinity recognition between streptavidin and biotin, which led to the proximity effect and brought B-GDNA3 and B-GDNA4 together to form a stable G-quadruplex structure. Upon the addition of hemin, the hemin/G-quadruplex DNAzyme could be formed to produce a DNAzyme-catalyzed CL signal (Figure 1B). The CL measurements indicated that the strong CL intensity only occurred in the mixture of two B-GDNAs, streptavidin, and hemin due to the formation of DNAzyme. With the protein array, the proximity-dependent formation of DNAzyme was further confirmed by incubating hemin solution, the mixture of hemin and CEA, the mixture of hemin and GDNA2-Ab2, and the mixture of hemin, CEA, and GDNA2-Ab2 on the sensing sites, respectively. The bright spot with strong CL intensity was only observed on the sensing site incubated with three components (Figure 1C), demonstrating the formation of DNAzyme to trigger the CL emission.

**Kinetic of CL Reaction.** The kinetic behavior of the CL reaction catalyzed by the generated DNAzyme on the array was examined with a static method (Figure 1D). The CL reaction occurred immediately upon the addition of CL substrates. The CL intensity increased quickly to the maximum value within 2 min and then slowly decreased to 80% of the maximum value after 6 min. Compared with the homogeneous DNAzyme-luminol- $\text{H}_2\text{O}_2$  CL reaction, the present system showed slower

CL reaction kinetics. This result was mainly due to the array-based heterogeneous reaction in which the CL reaction kinetics was controlled by the diffusion process. Here, in order to collect CL signal effectively, an exposure time of 5 min was used for CCD dynamic integration.

**Optimization of Assay Conditions.** In this work, the sequences of GDNA1 and GDNA2 were designed according to the previous works.<sup>30,49,50</sup> The concentration of GDNA1 used for the array preparation was first optimized. As shown in Figure 2A, the low concentration of GDNA1 showed a low CL

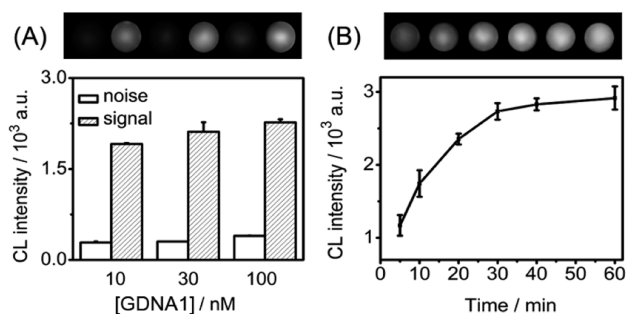


**Figure 2.** Optimization of (A) GDNA1 concentration at 160 ng mL<sup>-1</sup> CEA and (B) incubation time at 1.6 μg mL<sup>-1</sup> CEA.

signal, suggesting the array prepared with low concentration of GDNA1 was insufficient to capture the target protein for forming DNAzyme. On the contrary, the high GDNA1 concentration caused a high density of GDNA1 on the array, which led to the nonspecific absorption of hemin and thus increased the noise. Considering the highest S/N, 30 nM of GDNA1 was used for the array preparation.

The assay performance depended on the incubation time for the immunoreaction and DNAzyme formation. Thus, the effect of incubation time on the CL signal was examined at 1.6 μg mL<sup>-1</sup> CEA (Figure 2B). The CL response increased with the increasing incubation time and trended to a maximum value at 30 min, indicating the saturated formation of immunocomplex as well as the DNAzyme. Thus, 30 min was selected for the CLIA.

**CLIA of CEA.** In the presence of CEA, GDNA2-Ab2, and hemin on the GDNA1-Ab1 immobilized sensing site, the sandwich immunocomplex was formed among Ab1, CEA, and Ab2, which caused the close proximity of GDNA1 and GDNA2 to in situ generate the peroxidase-mimicking hemin-G-quadruplex DNAzyme for the CL imaging assay of CEA. Under the optimal conditions, the brightness of the sensing spot on the array increased with the increasing concentration of CEA. The CL intensity was proportional to the logarithm value of CEA concentration over the range of 0.16 ng mL<sup>-1</sup> to 1.6 μg mL<sup>-1</sup> with a limit of detection down to 0.15 ng mL<sup>-1</sup> (~0.5 pM) corresponding to the signal of 3SD (Figure 3A), which was lower than those of immunoassays using hemin/G-quadruplex DNAzyme as tag.<sup>51,52</sup> The pM detection limit with a wide detection range was comparable to another assay based on the proximity-dependent homogeneous chemiluminescence bioassay.<sup>53</sup> Due to the one-step proximity-dependent formation of DNAzyme, the proposed CLIA could be carried out within 40 min, which led to a throughput of 72 tests per hour for CEA measurement on a 48-cell sensing array.

**Evaluation of Cross-Reactivity, Stability, and Clinical Application.** The cross-reactivity between the CEA array and nonspecific analytes was evaluated by incubating the CEA array

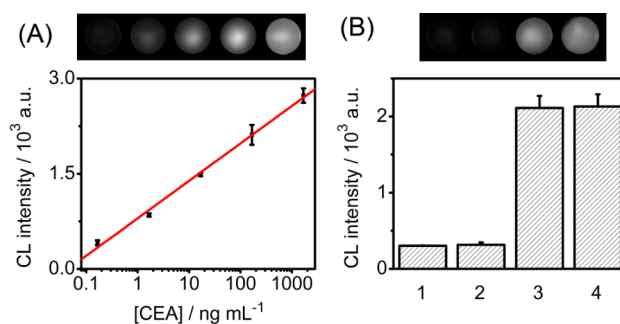


**Figure 3.** (A) CL image of CEA at 0.16, 1.6, 16, 160, 1600 ng mL<sup>-1</sup> and corresponding calibration curve. (B) CL responses of CEA sensing array incubated with the mixture of (1) 1 μM hemin and 20 nM Ab2-GDNA2, (2) (1) + 160 U mL<sup>-1</sup> CA 125 and CA 199, (3) (1) + 160 ng mL<sup>-1</sup> CEA, and (4) (1) + 160 ng mL<sup>-1</sup> CEA + 160 U mL<sup>-1</sup> CA 125 and CA 199.

with the mixture of hemin and GDNA2-Ab2 containing different antigens (Figure 3B). As expected, the strong CL intensity was observed on the sensing sites incubated with the solutions containing CEA, indicating negligible cross-reactivity and nonspecific binding in the proposed CLIA. After the CEA array was stored for a period of 30 days, the CL response was 94.4% of its initial response, exhibiting an acceptable stability of the protein array.

To evaluate the analytical reliability and application potential of the array-based CLIA, 5 assay results of CEA in human serum samples from cancer patients were obtained by the proposed method to compare with the reference values obtained by commercial ECL testing. The serum samples were detected directly without any dilution and treatment. As shown in Table 2, the assay results of CEA were in good

**Table 2.** Assay Results of CEA in Clinical Serum Samples Using the Proposed and Reference Methods

	sample no.				
	1	2	3	4	5
proposed method (ng mL <sup>-1</sup> )	248.1	1.95	49.32	5.82	1.08
reference method (ng mL <sup>-1</sup> )	231.6	2.03	49.91	5.75	1.03
relative error (%)	7.1	-3.9	-1.2	1.2	4.9

agreement with the reference values with relative errors less than 7.1%. Overall, the good accuracy along with the convenient operation and less sample consumption provided potential application in practical diagnosis.

**CLIA of Thrombin.** Similar to the antibody/antigen/antibody sandwich recognition, aptamer/target/aptamer recognition could also be applied to detect aptamer-responsible proteins with the proposed CLIA. Using thrombin as a model and taking the G-rich sequences of aptamer 15 itself into account,<sup>54</sup> the aptamer-based probes of Apt-P1 and Apt-P2 were single DNA strands containing both fragments of G-quadruplex and aptamer 15. The presence of thrombin triggered the formation of Apt-P1/thrombin/Apt-P2 complex and G-quadruplex structure on the Apt-P1 array, which subsequently produced the DNAzyme to catalyze the CL reaction for CLIA of thrombin (Figure 4A). Actually, the formation of Apt-P1/thrombin/Apt-P2 complex itself could also produce G-quadruplex structure due to the G-rich sequence of Apt-P1 and Apt-P2, which was demonstrated using the probes containing only the fragment of aptamer 15

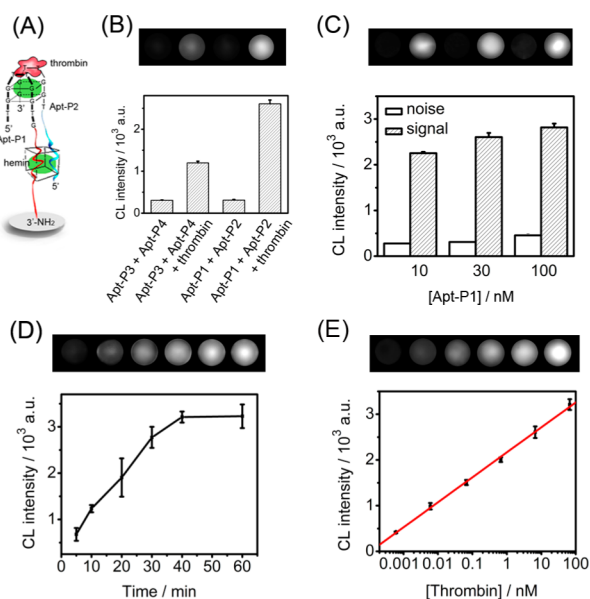


**Figure 4.** (A) Formation of DNAzyme on Apt-P1 array. (B) CL intensities of CLIA using Apt-P3/Apt-P4 and Apt-P1/Apt-P2 in the absence and presence of 6.7 nM thrombin. Optimization of (C) Apt-P1 concentration for array preparation at 6.7 nM thrombin and (D) incubation time for formation of DNAzyme at 67 nM thrombin. (E) CL image of thrombin at  $6.7 \times 10^{-4}$ ,  $6.7 \times 10^{-3}$ , 0.067, 0.67, 6.7, and 67 nM and the corresponding calibration curve.

(Apt-P3 and Apt-P4) (Figure 4B). In the absence of GDNA, the Apt-P3/thrombin/Apt-P4 complex in the presence of hemin produced strong CL emission, which was about half of the CL emission of the Apt-P1/thrombin/Apt-P2 system. Thus, the formation of Apt-P1/thrombin/Apt-P2 complex produced two G-quadruplex structures, leading to higher sensitivity.

To obtain the standard curve for detection of thrombin, the Apt-P1 concentration for preparation of Apt-P1 array was optimized to be 30 nM (Figure 4C), at which the incubation time for forming the hemin/G-quadruplex DNAzyme to trigger the maximum CL emission was chosen to be 40 min (Figure 4D). The linear range for thrombin detection was from 0.67 pM to 67 nM, and the detection limit was 0.49 pM (Figure 4E).

## CONCLUSIONS

This work proposed a simple array-based chemiluminescence imaging method for high throughput detection of protein targets via in situ proximity-dependent formation of DNAzyme on GDNA-Ab or GDNA-aptamer array. In the presence of target protein and another GDNA-probe, the formation of sandwich complex led to the proximity effect to in situ produce the hemin-G-quadruplex DNAzyme, which subsequently catalyzed the CL reaction to generate the CL signal. As the proximity-dependent DNAzyme formation could be carried out in one step, the array-based CLIA was simple and could be completed within 40 min, providing a throughput of 72 tests per hour for protein measurement. The proposed CLIA method showed wide detection ranges and low limits of detection without any signal amplification. By changing the pair of affinity probes, this method could be easily expanded to detect other protein analytes. The advantages of simple operation, high throughput and sensitivity, good versatility,

and acceptable selectivity and accuracy indicated good practicability of this method in bioanalysis.

## AUTHOR INFORMATION

### Corresponding Author

\*Phone/Fax: +86-25-83593593. E-mail: hxju@nju.edu.cn.

### Notes

The authors declare no competing financial interest.

## ACKNOWLEDGMENTS

This work is supported by the National Basic Research Program (2010CB732400), National Natural Science Foundation of China (21135002, 21121091, and 21105046), PhD Fund for Young Teachers (20110091120012), the Leading Medical Talents Program from the Department of Health of Jiangsu Province, and Science Foundation of Jiangsu (BK2011552 and BL2013036).

## REFERENCES

- (1) Sakamoto, S.; Omagari, K.; Kita, Y.; Mochizuki, Y.; Naito, Y.; Kawata, S.; Matsuda, S.; Itano, O.; Jinno, H.; Takeuchi, H.; Yamaguchi, Y.; Kitagawa, Y.; Handa, H. *Clin. Chem.* **2014**, *60*, 610–620.
- (2) Chen, L. C.; Zeng, X. T.; Si, P.; Chen, Y. M.; Chi, Y. W.; Kim, D. H.; Chen, G. N. *Anal. Chem.* **2014**, *86*, 4188–4195.
- (3) Chen, W. J.; Zheng, L. Y.; Wang, M. L.; Chi, Y. W.; Chen, G. N. *Anal. Chem.* **2013**, *85*, 9655–9663.
- (4) Lang, Q. L.; Wang, F.; Yin, L.; Liu, M. J.; Petrenko, V. A.; Liu, A. H. *Anal. Chem.* **2014**, *86*, 2767–2774.
- (5) Michels, D. A.; Tu, A. W.; McElroy, W.; Voehringer, D.; Salas-Solano, O. *Anal. Chem.* **2012**, *84*, 5380–5386.
- (6) Zong, C.; Wu, J.; Wang, C.; Ju, H. X.; Yan, F. *Anal. Chem.* **2012**, *84*, 2410–2415.
- (7) Niazov, T.; Pavlov, V.; Xiao, Y.; Gill, R.; Willner, I. *Nano Lett.* **2004**, *4*, 1683–1687.
- (8) Bi, S.; Ji, B.; Zhang, Z. P.; Zhang, S. S. *Chem. Commun.* **2013**, *49*, 3452–3454.
- (9) Du, D.; Wang, J.; Lu, D. L.; Dohnalkova, A.; Lin, Y. H. *Anal. Chem.* **2011**, *83*, 6580–6585.
- (10) Akter, R.; Rahman, M. A.; Rhee, C. K. *Anal. Chem.* **2012**, *84*, 6407–6415.
- (11) Bi, S.; Zhou, H.; Zhang, S. S. *Biosens. Bioelectron.* **2009**, *24*, 2961–2966.
- (12) Zhang, Q. Z.; Zhao, B.; Yan, J.; Song, S. P.; Min, R.; Fan, C. H. *Anal. Chem.* **2011**, *83*, 9191–9196.
- (13) Mani, V.; Chikkaveeraiah, B. V.; Patel, V.; Gutkind, J. S.; Rusling, J. F. *ACS Nano* **2009**, *3*, 585–594.
- (14) Du, D.; Wang, L. M.; Shao, Y. Y.; Wang, J.; Engelhard, M. H.; Lin, Y. H. *Anal. Chem.* **2011**, *83*, 746–752.
- (15) Yi, H. Y.; Xu, W. J.; Yuan, Y. L.; Bai, L. J.; Wu, Y. M.; Chai, Y. Q.; Yuan, R. *Biosens. Bioelectron.* **2014**, *54*, 415–420.
- (16) Ge, S. G.; Liu, W. Y.; Ge, L.; Yan, M.; Yan, J. X.; Huang, J. D.; Yu, J. H. *Biosens. Bioelectron.* **2013**, *49*, 111–117.
- (17) Tang, D. P.; Su, B. L.; Tang, J.; Ren, J. J.; Chen, G. N. *Anal. Chem.* **2010**, *82*, 1527–1534.
- (18) Zeng, Y. P.; Hu, J.; Long, Y.; Zhang, C. Y. *Anal. Chem.* **2013**, *85*, 6143–6150.
- (19) Bi, S.; Zhao, T. T.; Luo, B. Y.; Zhu, J. J. *Chem. Commun.* **2013**, *49*, 6906–6908.
- (20) Wang, L. J.; Zhang, Y.; Zhang, C. Y. *Anal. Chem.* **2013**, *85*, 11509–11517.
- (21) Tang, L. H.; Liu, Y.; Ali, M. M.; Kang, D. K.; Zhao, W. A.; Li, J. H. *Anal. Chem.* **2012**, *84*, 4711–4717.
- (22) Xu, J.; Wu, J.; Zong, C.; Ju, H. X.; Yan, F. *Anal. Chem.* **2013**, *85*, 3374–3379.
- (23) Liu, J. W.; Cao, Z. H.; Lu, Y. *Chem. Rev.* **2009**, *109*, 1948–1998.
- (24) Kolpashchikov, D. M. *J. Am. Chem. Soc.* **2008**, *130*, 2934–2935.

- (25) Deng, M. G.; Zhang, D.; Zhou, Y. Y.; Zhou, X. *J. Am. Chem. Soc.* **2008**, *130*, 13095–13102.
- (26) Nakayama, S.; Sintim, H. O. *J. Am. Chem. Soc.* **2009**, *131*, 10320–10333.
- (27) Hou, T.; Wang, X. Z.; Liu, X. J.; Liu, S. F.; Du, Z. F.; Li, F. *Analyst* **2013**, *138*, 4728–4731.
- (28) Shimron, S.; Wang, F.; Orbach, R.; Willner, I. *Anal. Chem.* **2012**, *84*, 1042–1048.
- (29) Wang, F.; Orbach, R.; Willner, I. *Chem.—Eur. J.* **2012**, *18*, 16030–16036.
- (30) Freeman, R.; Liu, X. Q.; Willner, I. *J. Am. Chem. Soc.* **2011**, *133*, 11597–11604.
- (31) Zhu, J. B.; Yang, X.; Zhang, L. B.; Zhang, L. L.; Lou, B. H.; Dong, S. J.; Wang, E. K. *Chem. Commun.* **2013**, *49*, 5459–5461.
- (32) Fredriksson, S.; Dixon, W.; Ji, H.; Koong, A. C.; Mindrinos, M.; Davis, R. W. *Nat. Methods* **2007**, *4*, 327–329.
- (33) Hu, J. M.; Wang, T. Y.; Kim, J.; Shannon, C.; Easley, C. J. *J. Am. Chem. Soc.* **2012**, *134*, 7066–7072.
- (34) Li, J. J.; Zhong, X. Q.; Zhang, H. Q.; Le, X. C.; Zhu, J. J. *Anal. Chem.* **2012**, *84*, 5170–5174.
- (35) Ren, K. W.; Wu, J.; Yan, F.; Ju, H. X. *Sci. Rep.* **2014**, *4*, 4360.
- (36) Zhang, H. Q.; Li, F.; Dever, B.; Wang, C.; Li, X. F.; Le, X. C. *Angew. Chem., Int. Ed.* **2013**, *52*, 10698–10705.
- (37) Nong, R. Y.; Wu, D.; Yan, J. H.; Hammond, M.; Gu, G. J.; Kamali-Moghaddam, M.; Landegren, U.; Darmanis, S. *Nat. Protoc.* **2013**, *8*, 1234–1248.
- (38) Gomez, D.; Shankman, L. S.; Nguyen, A. T.; Owens, G. K. *Nat. Methods* **2013**, *10*, 171–179.
- (39) Lundberg, M.; Eriksson, A.; Tran, B.; Assarsson, E.; Fredriksson, S. *Nucleic Acids Res.* **2011**, *39*, No. e102.
- (40) Zieba, A.; Wahlby, C.; Hjelm, F.; Jordan, L.; Berg, J.; Landegren, U.; Pardali, K. *Clin. Chem.* **2010**, *56*, 99–110.
- (41) Weibrecht, I.; Lundin, E.; Kiflemariam, S.; Mignardi, M.; Grundberg, I.; Larsson, C.; Koos, B.; Nilsson, M.; Söderberg, O. *Nat. Protoc.* **2013**, *8*, 355–372.
- (42) Li, F.; Zhang, H. Q.; Lai, C.; Li, X. F.; Le, X. C. *Angew. Chem., Int. Ed.* **2012**, *51*, 9317–9320.
- (43) Zong, C.; Wu, J.; Liu, M. M.; Yang, L. L.; Liu, L.; Yan, F.; Ju, H. X. *Anal. Chem.* **2014**, *86*, 5573–5578.
- (44) Donhauser, S. C.; Niessner, R.; Seidel, M. *Anal. Chem.* **2011**, *83*, 3153–3160.
- (45) Roda, A.; Mirasoli, M.; Dolci, L. S.; Buragina, A.; Bonvicini, F.; Simoni, P.; Guardigli, M. *Anal. Chem.* **2011**, *83*, 3178–3185.
- (46) Ruan, M.; Niu, C. G.; Qin, P. Z.; Zeng, G. M.; Yang, Z. H.; He, H.; Huang, J. *Anal. Chim. Acta* **2010**, *664*, 95–99.
- (47) Söderberg, O.; Gullberg, M.; Jarvius, M.; Ridderstråle, K.; Leuchowius, K.; Jarvius, J.; Wester, K.; Hydbring, P.; Bahram, F.; Larsson, L. G.; Landegren, U. *Nat. Methods* **2006**, *12*, 995–1000.
- (48) Balagurumoorthy, P.; Brahmachari, S.; Mohanty, D.; Bansal, M.; Sasisekharan, V. *Nucleic Acids Res.* **1992**, *20*, 4061–4067.
- (49) Li, F.; Lin, Y. W.; Le, X. C. *Anal. Chem.* **2013**, *85*, 10835–10841.
- (50) Zhang, Y. L.; Huang, Y.; Jiang, J. H.; Shen, G. L.; Yu, R. Q. *J. Am. Chem. Soc.* **2007**, *129*, 15448–15449.
- (51) Zhu, Y. Y.; Xu, L. G.; Ma, W.; Chen, W.; Yan, W. J.; Kuang, H.; Wang, L. B.; Xu, C. L. *Biosens. Bioelectron.* **2011**, *26*, 4393–4398.
- (52) Zhou, W. H.; Zhu, C. L.; Lu, C. H.; Guo, X. C.; Chen, F. R.; Yang, H. H.; Wang, X. R. *Chem. Commun.* **2009**, *45*, 6845–6847.
- (53) Akhavan-Tafti, H.; Binger, D. G.; Blackwood, J. J.; Chen, Y.; Creager, R. S.; Silva, R. D.; Eickholt, R. A.; Gaibor, J. E.; Handley, R. S.; Kapsner, K. P.; Lopac, S. K.; Mazelis, M. E.; McLernon, T. L.; Mendoza, J. D.; Odegaard, B. H.; Reddy, S. G.; Salvati, M.; Schoenfelner, B. A.; Shapir, N.; Shelly, K. R.; Todtleben, J.; Wang, G. P.; Xie, W. H. *J. Am. Chem. Soc.* **2013**, *135*, 4191–4194.
- (54) Liu, X. Q.; Freeman, R.; Golub, E.; Willner, I. *ACS Nano* **2011**, *5*, 7648–7655.